

# Strain on the San Andreas Fault Near Palmdale, California: Rapid, Aseismic Change

**Abstract.** Frequently repeated strain measurements near Palmdale, California, during the period from 1971 through 1980 indicate that, in addition to a uniform accumulation of right-lateral shear strain (engineering shear, 0.35 microradian per year) across the San Andreas fault, a 1-microstrain contraction perpendicular to the fault that accumulated gradually during the interval 1974 through 1978 was aseismically released between February and November 1979. Subsequently (November 1979 to March 1980), about half of the contraction was recovered. This sequence of strain changes can be explained in terms of south-southwestward migration of a slip event consisting of the south-southwestward movement of the upper crust on a horizontal detachment surface at a depth of 10 to 30 kilometers. The large strain change in 1979 corresponds to the passage of the slip event beneath the San Andreas fault.

The U.S. Geological Survey monitors strain accumulation in southern California, using very precise electro-optical surveys of trilateration networks (1). The tensor strain accumulation in the network can be calculated from the average strains of the 30 or more individual lines in the trilateration network. The measurement is essentially no different from the laboratory technique of placing finite-sized strain gages on test specimens to determine strain. Indeed, the area of our trilateration networks is in approximately the same proportion to the study area (southern California) as strain gage area to specimen size in the laboratory.

The Palmdale trilateration network

(Fig. 1) spans the San Andreas fault about 60 km north of Los Angeles. A plot of the strain accumulation observed there as a function of time is shown in Fig. 2. The strain components in Fig. 2 have been referred to a coordinate system in which the 1 axis is directed to the east-southeast along the strike of the San Andreas fault and the 2 axis is directed north-northeast perpendicular to the fault (inset in Fig. 2). The shear strain component  $\gamma'_2$  (equal to twice the tensor component  $\epsilon'_{12}$ ) measures right-lateral shear across the San Andreas fault, the expected mode of strain accumulation. Within the precision of measurement, the accumulation of  $\gamma'_2$  shown in Fig. 2 is

linear in time, indicating a uniform shear strain rate  $\dot{\gamma}'_2 = 0.35 \pm 0.02 \mu\text{rad}/\text{year}$ . This accumulation of shear strain is readily explained by conventional models of the San Andreas fault (2). Although the along-strike component of strain  $\epsilon'_{11}$  shows marginally significant fluctuations (particularly in 1979), all the observed strains remain within 2 standard deviations of the mean value. The anomalous strain accumulation is shown principally in  $\epsilon'_{22}$ , the component normal to the fault: a steadily increasing contraction during the period from 1974 through 1978, a sudden extension of 1.2  $\mu\text{strain}$  between February and October 1979, and a rapid contraction in late 1979 and early 1980 followed by an extension before mid-1980. It is not completely clear that these 1980 changes are real, as the changes are comparable to the errors in measurement.

The sudden change in strain observed between the surveys of 1979.2 and 1979.8 was so surprising that we have attempted to verify it by several means. First, we had the 1979.8 survey repeated 1 month later (1979.9) with an entirely different set of instruments. The agreement between the two surveys was satisfactory (Fig. 2). Second, by comparing different surveys and surveys of different portions of the network, we were able to

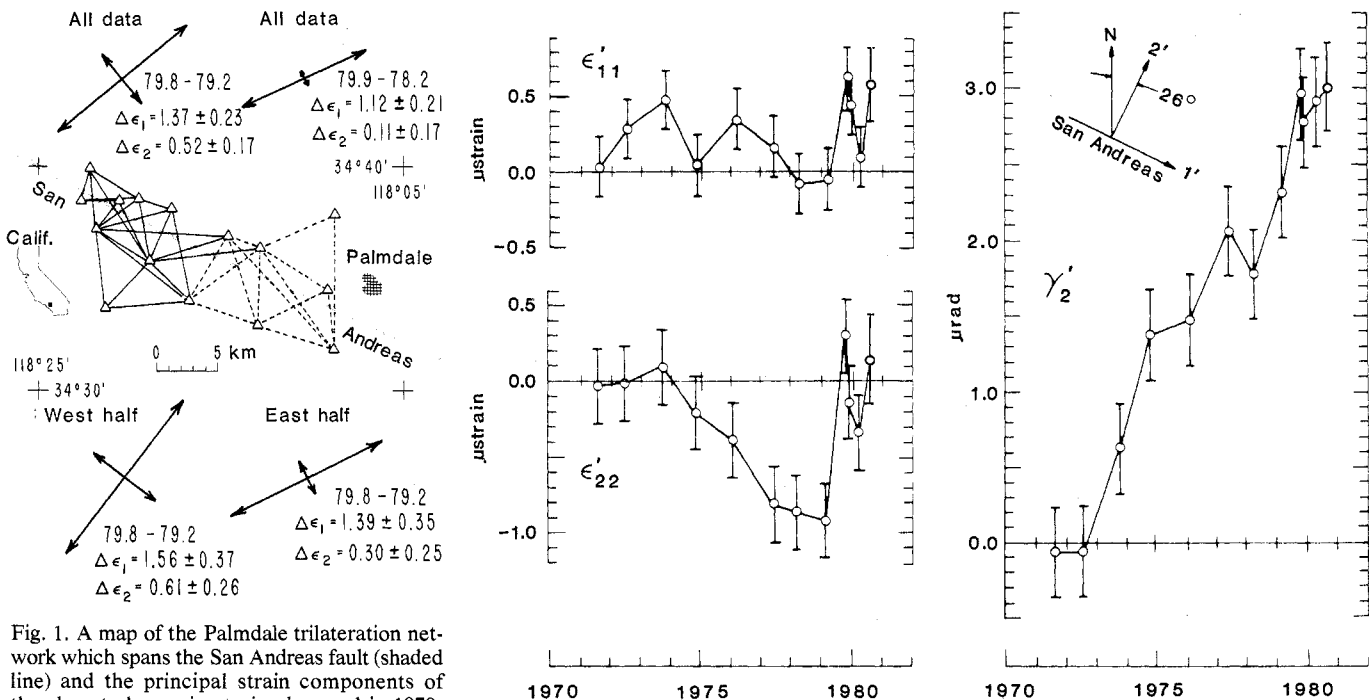


Fig. 1. A map of the Palmdale trilateration network which spans the San Andreas fault (shaded line) and the principal strain components of the abrupt change in strain observed in 1979. At the top are shown the strain changes deduced from the complete Palmdale trilateration network for the two intervals 1979.2 to 1979.8 and 1978.2 to 1979.9, and at the bottom are shown the strain changes for the interval 1979.2 to 1979.8 as deduced from the west and east halves (solid and dashed lines, respectively, in the network diagram) of the Palmdale network. The quoted uncertainties in the strains are standard deviations. Fig. 2. Strain accumulation near Palmdale, California, as a function of time as deduced from surveys of the Palmdale trilateration network for the interval 1971 through 1980. The strain components are referred to a coordinate system in which the 1 axis is directed S64°E along the strike of the San Andreas fault and the 2 axis is directed N26°E perpendicular to the fault. The tensor strain components are denoted by  $\epsilon'_{ij}$  and the engineering shear strain ( $2\epsilon'_{12}$ ) by  $\gamma'_2$ . The error bars represent 1 standard deviation on either side of the plotted point.

show that the strain jump was not associated solely with one particular survey or with anomalous motion in only one part of the network. For example, in Fig. 1 the principal strain components of the strain jump are shown as calculated in several different ways. At the top are shown the principal strains calculated for two independent intervals: 1979.2 to 1979.8 on the left and 1978.2 to 1979.9 on the right. In the lower part are shown the principal strain components for the 1979.2 to 1979.8 strain jump as calculated independently from the west and east halves of the network. In all cases the principal strains agree within the observational errors. Our instrumentation is apparently not at fault because other networks in southern California surveyed with the same instruments over the same time interval did not show similar strain jumps.

The anomalous strain jump shown in Figs. 1 and 2 may be associated with other geophysical anomalies (radon, gravity, and resistivity) observed in southern California during 1979 (3). In particular, a very anomalous deformation detected by a very-long-baseline interferometry antenna at Pasadena (45 km south of the Palmdale network) appears to exhibit appreciable coherence with the 1979 Palmdale strain jump and its subsequent relaxation (4). (The 1979.8 survey of the Palmdale network was in fact prompted by an early report of that deformation.) However, in the following paragraphs we will concentrate on a simple model that explains our own observations of the anomalous strain change near Palmdale. Whether that model, or indeed any simple model, can explain all of the reported southern California anomalies remains to be investigated.

The anomalous strain ( $\epsilon'_{22}$ ) observed near Palmdale (Fig. 2) can be explained in terms of a simple two-dimensional model of an edge dislocation in an elastic half space. The Burgers vector  $b$  of the edge dislocation is taken to be parallel to the free surface, and the dislocation is supposed to move along a horizontal glide plane in the direction of the Burgers vector (inset in Fig. 3). The deformation of the surface of the half space due to the presence of the dislocation is easily calculated (5), and plots of the horizontal strain  $\partial u/\partial x$  and vertical displacement (uplift)  $v$  are given as a function of the horizontal distance from the dislocation in Fig. 3. The dislocation model corresponds to the geologic situation in which the upper part of the crust ( $-a < y < 0$ ) to the right of the dislocation ( $x > 0$ ) has slipped an amount  $b$  to the left over a

horizontal plane of detachment at depth  $a$  (inset in Fig. 3). To use this model to explain the changes in  $\epsilon'_{22}$  shown in Fig. 2, we suppose that the dislocation line strikes N64°W so that the inset diagram in Fig. 3 represents a vertical section perpendicular to the San Andreas fault (that is,  $x$  increases in the direction N26°E). The strain  $\partial u/\partial x$  in Fig. 3 then corresponds to  $\epsilon'_{22}$  in Fig. 2. We now suppose that the dislocation was located five or six fault depths north-northeast of the Palmdale network in 1974 (that is, Palmdale would be located at  $x/a = -5.5$  in Fig. 3) and migrates to the south-southwest at the rate of about one fault depth  $a$  each year so that it passes beneath the Palmdale network in mid-1979. This uniform rate of migration establishes an equivalence between the abscissa  $x$  in Fig. 3 and time. That is, Fig. 3 may be read as a plot of deformation versus time with the origin corresponding to 1979.5, each unit of the abscissa corresponding to about 1 year and time increasing to the right. A coincidence between the ordinates in Figs. 2 and 3 is obtained by requiring

$$b = 7.5 \times 10^{-6} a$$

and

$$v_{\max} = 2.5 \times 10^{-6} a$$

that is, 75 mm of slip and 25 mm of maximum uplift for each 10 km of fault depth  $a$ . With this scaling, a good fit to the observed accumulation of  $\epsilon'_{22}$  through March 1980 is obtained, but the July 1980 measurement deviates from the strain predicted by the model. The available leveling data are not adequate to detect the uplifts predicted by the model, but

leveling along a 15-km north-south line through Palmdale in 1965, 1968, 1971, and 1974 indicates reversals in tilt of the magnitude predicted for the 1979 event (2), perhaps due to an earlier slip migration.

The existence of a horizontal detachment surface (or zone) at the bottom of the lithosphere is, of course, implicit in plate tectonic theory. Whether the detachment surface postulated in this report coincides with the bottom of the tectonic plate is problematic. Generally, the lithosphere is thought to be 50 or more kilometers thick, but there is some evidence that the plate thickness in southern California is appreciably less, the detachment surface being perhaps as shallow as 10 to 30 km. Such a shallow detachment surface has been suggested to account for the absence of earthquakes deeper than about 15 km (6), the broad heat-flow anomaly along the San Andreas fault (7), the focal mechanisms of certain earthquakes that appear to require slip on nearly horizontal fault planes (8), and the absence of an offset in a deep structure continuous across the San Andreas fault beneath the Transverse Ranges (9).

A similar migration of slip events on a low-angle thrust dipping northward beneath the Transverse Ranges was suggested by Thatcher (10) to account for vertical deformation observed during the southern California uplift, and earlier Castle *et al.* (11) suggested that episodic uplift near the epicenter of the San Fernando earthquake but prior to the earthquake itself could be attributed to creep at depth on the thrust fault. The explanation advanced here to explain the

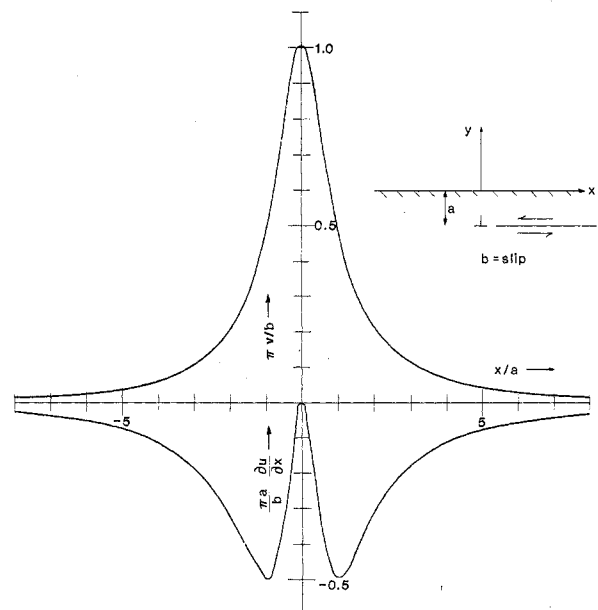


Fig. 3. The vertical displacement  $v$  (upper curve) and horizontal strain  $\partial u/\partial x$  (lower curve) at the free surface produced by an edge dislocation buried at depth  $a$  in an elastic half space. The Burgers vector  $b$  of the dislocation is parallel to the free surface.

anomalous strain observed near Palmdale does not differ significantly from these earlier explanations. The Palmdale strain anomaly could as well be explained by migration of slip on a low-angle thrust as a horizontal detachment plane. Indeed, continued slip on a horizontal detachment plane must ultimately be relieved along a thrust plane, and, if the detachment plane exists, it is likely that it is coupled to the system of thrust faults beneath the Transverse Ranges, perhaps as one great listric fault.

J. C. SAVAGE  
W. H. PRESCOTT  
M. LISOWSKI  
N. E. KING

U.S. Geological Survey,  
345 Middlefield Road,  
Menlo Park, California 94025

#### References

1. J. C. Savage, W. H. Prescott, M. Lisowski, N. King, *Science* **202**, 883 (1978); J. C. Savage and W. H. Prescott, *J. Geophys. Res.* **78**, 6001 (1973).
2. W. H. Prescott and J. C. Savage, *J. Geophys. Res.* **81**, 4901 (1976).
3. J. H. Whitcomb, *Eos Trans. Am. Geophys. Union* **61**, 368 (1980).
4. A. E. Neill, *ibid.* **60**, 810 (1979); oral presentation at the American Geophysical Union meetings, San Francisco, December 1979.
5. T. Mura, *Adv. Mater. Res.* **3**, 1 (1968).
6. D. L. Anderson, *Sci. Am.* **225**, 53 (November 1971).
7. A. H. Lachenbruch and J. H. Sass, in *Proceedings of the Conference on Tectonic Problems of the San Andreas Fault System*, R. L. Kovach and A. Nur, Eds. (Department of Geological Sciences, Stanford University, Stanford, Calif., 1973), p. 192.
8. D. Hadley and H. Kanamori, *Bull. Seismol. Soc. Am.* **68**, 1449 (1978).
9. ———, *Geol. Soc. Am. Bull.* **88**, 1469 (1977).
10. W. Thatcher, *Science* **194**, 691 (1976); J. B. Rundle and W. Thatcher, *Bull. Seismol. Soc. Am.* **70**, 1869 (1980).
11. R. O. Castle, J. N. Alt, J. C. Savage, E. I. Balazs, *Geology* **2**, 61 (1974).

6 June 1980; revised 27 October 1980

## Cellulose Metabolism by the Flagellate *Trichonympha* from a Termite Is Independent of Endosymbiotic Bacteria

**Abstract.** Continuous axenic cultures were established of *Trichonympha sphaerica*, a cellulose-digesting symbiotic protozoon in the gut of a termite. The cultured flagellates harbored no endosymbiotic bacteria and metabolized cellulose to acetate, carbon dioxide, and hydrogen. Thus, the cellulolytic activity of this flagellate is an inherent property and is not dependent on endosymbiotic bacteria.

Flagellated Protozoa in the order Hypermastigida are mostly large, structurally complex, cellulose-digesting symbiotes in the intestines of termites and the wood-feeding roach *Cryptocercus* (1-3). These insects live on a diet of cellulose but possess insufficient cellulolytic

activity, thereby rendering them dependent on their flagellates for cellulose digestion (1-3). Degradation of cellulose by the flagellates provides the host with usable end products, which have been identified as acetate (plus CO<sub>2</sub> and H<sub>2</sub>) for flagellates from the termite *Zooter-*

*mopsis* (3). The origin of cellulolytic activity in the flagellates (4) is uncertain (2, 3) because they harbor endosymbiotic bacteria (5). Pierantoni (6) first postulated that bacteria living within termite flagellates are responsible for hydrolyzing cellulose to soluble sugars. This hypothesis, without experimental support (2, 3, 5), has nevertheless become quite popular.

Axenic cultivation of cellulose-digesting hypermastigote flagellates would preclude the involvement of living bacteria in flagellate cellulose metabolism. However, continuous cultivation of these flagellates under axenic conditions has not been achieved previously. Trager (7) obtained multiplication of *Trichonympha sphaerica* in primary cultures and first subcultures. A mixed population of flagellates, including hypermastigotes, from *Cryptocercus* have been grown in culture for extended periods (8). The sensitivity of these flagellates to oxygen (2, 3) and their possible complex nutritional requirements (3) have probably contributed to their neglect as candidates for detailed study in vitro. Axenic cultivation is now reported for a hypermastigote, *Trichonympha sphaerica*, from the western damp-wood termite *Zootermopsis* (9).

The culture technique used was that developed for axenic cultivation of a cellulose-digesting trichomonad flagellate (10). The anaerobic medium contained cellulose particles and heat-killed bacteria (11). In our study, the intestinal contents of *Zootermopsis* (12) were inoculated into the culture medium containing 250 units of penicillin and 250 μg of streptomycin per milliliter, and the inoculated cultures were incubated at 20°C. After 9 weeks, a mixed culture of *Trichonympha sphaerica*, *Trichomitopsis termopsidis*, and intestinal bacteria was obtained. To separate *T. sphaerica* from *T. termopsidis*, we selected 25 cells of the former from primary culture fluid with a micropipette, checked to ensure the absence of trichomonads, and then inoculated them into fresh medium with antibiotics. The flagellates multiplied to several hundred cells after 8 weeks; thereafter, they were subcultured about every 4 weeks. After several further passages, living extracellular bacteria were absent (13), and antibiotics were omitted from the medium. Flagellates typically increased tenfold after 4 weeks and reached about 150 cells per milliliter of medium. The cells were actively motile in culture and were filled with cellulose particles (Fig. 1a).

Since endosymbiotic bacteria have been reported in *T. sphaerica* (14), the

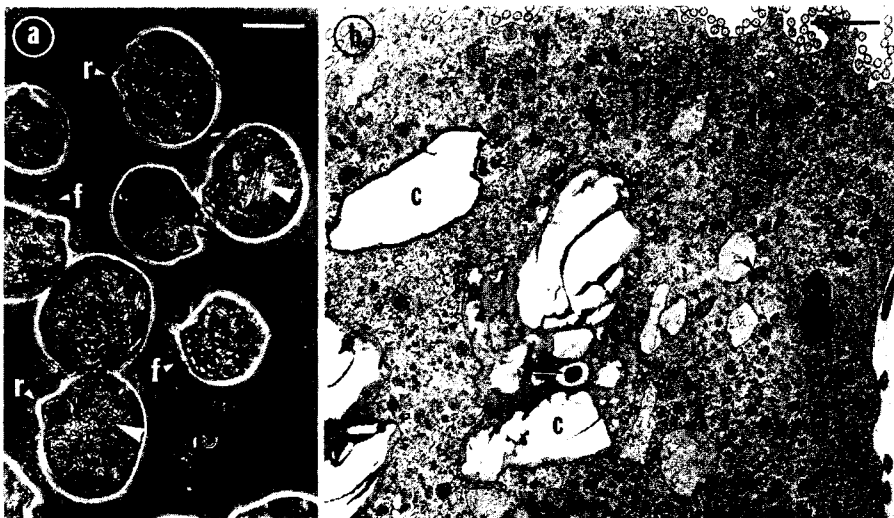


Fig. 1. *Trichonympha sphaerica* from axenic culture. (a) Light micrograph with phase contrast optics of cells fixed with glutaraldehyde. Each cell has an anterior rostrum (r), flagella (f), and cytoplasm containing many ingested cellulose particles (arrowheads). The bar represents 100 μm. (b) Electron micrograph of part of a cell showing the absence of endosymbiotic bacteria in the cytoplasm. The usual cytoplasmic organelles are present, including microbodies (small arrowheads) and food vacuoles containing cellulose particles (c) and a heat-killed food bacterium (large arrowhead). Bar represents 2 μm.